The transformation of the rotational energy of a Kerr black hole

OPEN ACCESS
IOP Publishing
Classical and Quantum Gravity
Class. Quantum Grav. **41** (2024) 135019 (22pp)
https://doi.org/10.1088/1361-6382/ad51c2

The transformation of the rotational energy of a Kerr black hole

Shu-Rui Zhang[1,2,3,*] **and Mikalai Prakapenia**[4,5]

[1] ICRANet-Ferrara, Dip. di Fisica e Scienze della Terra, Università degli Studi di Ferrara, Via Saragat 1, I–44122 Ferrara, Italy
[2] School of Astronomy and Space Science, University of Science and Technology of China, Hefei 230026, People's Republic of China
[3] CAS Key Laboratory for Research in galaxies and Cosmology, Department of Astronomy, University of Science and Technology of China, Hefei 230026, People's Republic of China
[4] ICRANet-Minsk, Institute of Physics, National Academy of Sciences of Belarus, Nezalezhnasci Av. 68-2, 220072 Minsk, Belarus
[5] Department of Theoretical Physics and Astrophysics, Belarusian State University, Nezalezhnasci Av. 4, 220030 Minsk, Belarus

E-mail: zhangsr@mail.ustc.edu.cn

Received 7 February 2024; revised 3 May 2024
Accepted for publication 29 May 2024
Published 12 June 2024

Abstract

This paper analyzes the feedback of the rotational energy extraction from a Kerr black hole (BH) by the 'ballistic method', i.e. the test particle decay in the BH ergosphere pioneered by Roger Penrose. The focus is on the negative energy counterrotating particles (which can be massive or massless) going in towards the horizon, and the feedback on the BH irreducible mass is assessed. Generally, the change in irreducible mass is a function of the conserved quantities of the particle. For an extreme Kerr BH and in the limit $\mu_1/M \to 0$, all the reduced transformable energy goes into the irreducible mass (i.e. $\Delta M_{\rm irr}/|E_1| \to \infty$), resulting in high irreversibility. The amount of extracted energy from the BH using test particles is much lower than the change of transformable energy. For non-extreme Kerr BHs, the effective potential of particle motion on the equatorial plane in Kerr spacetime is analyzed, and it is demonstrated that the Penrose process can only be undergone by BHs with a dimensionless spin $\hat{a} > 1/\sqrt{2}$ if the decay point coincides with the turning point. Based on that, the lower limit of the change in irreducible mass is provided as a function of the dimensionless spin of the BH. The significance of the increase in the irreducible mass of the BH during the energy extraction process is generally and concisely illustrated by introducing the concept of transformable energy

* Author to whom any correspondence should be addressed.

of the BH. The feedback from the Penrose process on the irreducible mass demonstrates the irreversibility of energy extraction and highlights that the total amount of energy that can be extracted from a BH is less than previously anticipated.

Keywords: classical general relativity, black hole, Penrose process, irreducible mass

1. Introduction

Longstanding issues include the mechanisms by which the extreme environments of BHs supply and transfer energy. The energy extraction from *ergosphere* of a Kerr black hole (BH) has attracted considerable attention in the current literature (e.g. [1, 2], and references therein). This paper provides a quantitative analysis of the feedback from the Penrose process on the irreducible mass, demonstrating the irreversibility of energy extraction and its impact on the total amount of energy that can be extracted from a BH. This subject is of academic and purely theoretical interest because the irreducible mass is linked to BH area or BH entropy. Additionally, it may have astrophysical implications concerning energy supply in extreme environments.

The Einstein equation is the cornerstone of modern gravitational physics, but it is nonlinear, making it difficult to solve. Nevertheless, Roy Kerr obtained an exact mathematical solution [3], which plays a central role in describing rotating objects in General Relativity. Subsequently, the discovery of the separability of the Hamilton–Jacobi equations for geodesics in the Kerr spacetime in terms of four conserved quantities allowed for the accurate analysis of the movement of test particles [4]. Moreover, the introduction of the effective potential [5, 6] further simplified the analysis of the physical trajectories of test particles with conserved energy and angular momentum on the equatorial plane. These contributions form the basis of Kerr BH physics formulation.

A practical application of these formalisms has led to the introduction of the concept of the ergosphere (see, e.g. [7]) and has paved the way for deriving the mass-energy formula of a Kerr BH. The research conducted by [8, 9] introduced the concept of irreducible mass $M_{\rm irr}$ and provided the mass-energy formula for a Kerr BH, given by

$$M^2 = M_{\rm irr}^2 + \frac{J^2}{4M_{\rm irr}^2}, \tag{1.1}$$

where $J^2/(4M_{\rm irr}^4) \leqslant 1$. Thus, the mass of a Kerr BH depends on two parameters: J and $M_{\rm irr}$. Additionally, [10] established the relationship between the irreducible mass and the surface area of the BH, as expressed in

$$A = 16\pi M_{\rm irr}^2. \tag{1.2}$$

Both the irreducible mass and surface area always increase during irreversible transformations. Furthermore, the surface area is linearly related to the entropy of the BH [11]. The work of Ruffini *et al* [12–15] related irreducible mass to extractable energy, but still did not properly consider the feedback effect brought by the growth of irreducible mass. In view of this, this paper deals with this issue in general and concisely.

Up to now, numerous methods and their corresponding extended research for extracting energy from BHs have been proposed [2, 15–22]. Especially, the challenge of using the Kerr BH as an energy source for astrophysical systems and it affect on irreduceble mass has been addressed in context of test magnetic field around a Kerr BH, with examples in the special

cases of GRBs and AGNs [23]. However, despite the ballistic Penrose process being the most fundamental one, the study of its influence on BHs has not been well-developed. Penrose and Floyd [24] pioneered the idea that ballistic particle fission can be used as a process of Kerr BH energy extraction. It was soon demonstrated that the Penrose process satisfies some constraints. In particular, Ward [25] provides the energy limit of the Penrose process, demonstrating that one cannot obtain significantly greater energies than those achievable through a similar breakup process in the absence of a BH. This paper introduces a new constraint on the decay position of the Penrose process, particularly when the decay point coincides with the turning point. Additionally, what remained incomplete at the time was the consideration of feedback regarding the irreducible mass resulting from the capture of a counterrotating test particle by the BH horizon. Both Penrose and Floyd [24] and Chandrasekhar [26] have mentioned that the Penrose process leads to an increase in the surface area of a BH, but a precise quantitative description is currently absent. For this reason, we re-examine this fundamental issue followed by location constraints in this paper. Meanwhile, the irreducible mass always increases for a BH in classical theory [9, 10]. Thus, it is fundamental to have a more direct exemplification of how to interact with this fundamental quantity, $M_{\rm irr}$.

In this paper, the main focus is on ballistic Penrose processes, where we establish and illustrate significant restrictions on the relationship between the released energy of a BH and the increase in the BH's irreducible mass. The paper is organized as follows: In section 2, the concept of transformable energy is presented to analyze various physical processes related to BHs in a unified and concise manner. Especially, it highlights the impact of the increase in the irreducible mass of the BH during the energy extraction process. This is a general discussion that is not based on a specific process. Section 3 provides the basic equations associated with the ballistic Penrose process, and establishes the constraints on the decay position when the decay point coincides with the turning point. Building upon this, we prove that the energy extracted from BH is less than the added irreducible mass for infalling particles both mass and massless in the extreme BH case in section 4. In section 5 we are not limited to extreme BHs, but for the general case. The lower limit of the change in irreducible mass as a function of the BH spin is provided. Lastly, the main conclusions are summarized in section 6. Unless otherwise specified, geometrical units ($G = c = 1$) are used in this study.

2. Transformable energy

Contrasting irreducible mass, we define the transformable energy of a BH as:

$$E_{\rm trans} = M - M_{\rm irr} = \left(1 - \sqrt{\frac{1+\sqrt{1-\hat{a}^2}}{2}}\right) M, \tag{2.1}$$

which is referred to as rotational energy in some works [27]. For the extreme Kerr BH, the $\hat{a} = 1$, and the transformable energy is $29.2893\%M$. Near the extreme value, the transformable energy decreases sharply with the decrease of spin. We are interested in the change in transformable energy because it can indicate how the 'reservoir' of BH energy shrinks or expands. Differentiating equation (2.1), it yields:

$$\Delta E_{\rm trans} = \Delta M - \Delta M_{\rm irr}. \tag{2.2}$$

Namely, the change of transformable energy depends not only on the change of BH mass but also on the increased amount of irreducible mass of BH. The symbol 'Δ' denotes the

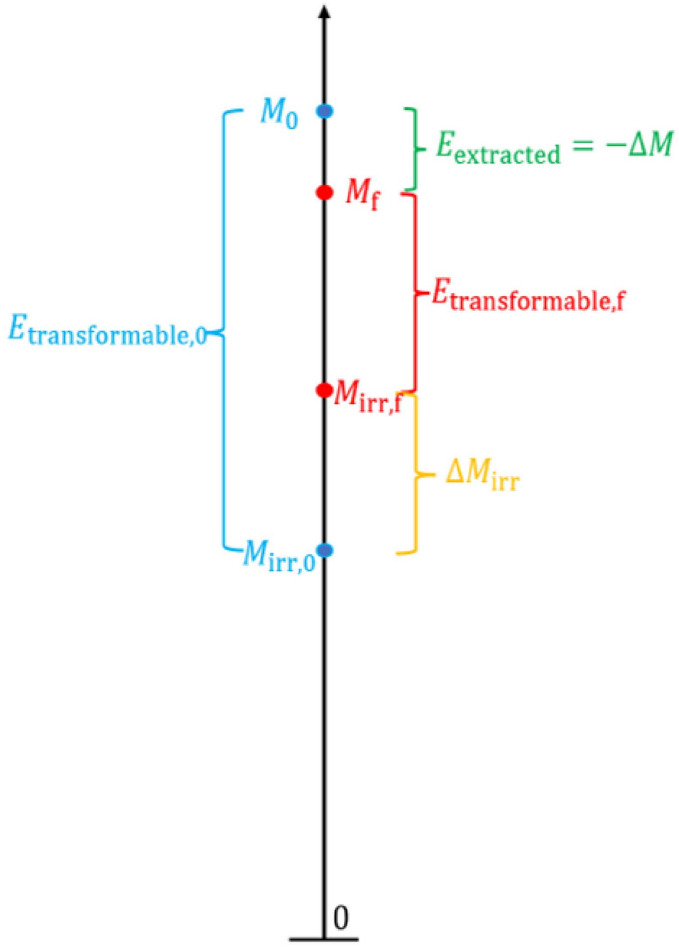

Figure 1. Schematic diagram of the changes in quantities of the BH during energy extraction processes. The initial state quantities of the BH are denoted by the blue color, while the final state quantities are represented by red. The green symbol indicates the amount of change in the mass of the BH, and the yellow symbol represents the amount of change in the irreducible mass. The process of energy extraction from the BH leads to a decrease in its mass. Simultaneously, the irreducible mass increases, both resulting in the reduction of transformable energy.

difference between the final and the initial physical quantities. For the infinitesimal process (i.e. test particles limit), the discrete symbol 'Δ' is substituted with the differential symbol 'd'. The quantity ΔM_{irr} can only have a positive value, whereas ΔM can take on positive, zero, and negative values, corresponding to normal BH accretion [28], the Pollock process [29, 30], and BH energy extraction, respectively.

For the energy extraction process, M decreases, but M_{irr} increases, so the transformable energy shrinks (see the further discussion and examples in the following section). Numerous studies also refer to equation (2.1) as extractable energy [12], and some argue that all transformable energy can be extracted [31]. However, this notion is fundamentally flawed as it disregards the feedback of the energy extraction process on the irreducible mass. As depicted in figure 1, only $-\Delta M$ represents the extracted energy according to the conservation of

energy, while the remaining portion (of the transformable energy change) is converted into irreducible mass. This implies that less energy can be extracted from a BH than previously expected. Therefore, this naturally leads us to investigate the quantitative increase in irreducible mass for specific energy extraction processes, particularly focusing on the fundamental Penrose process.

3. Basic equations and location constraints for Penrose processes

The preceding discussion provides a general overview. We now shift our focus to a specific yet fundamental energy extraction process known as the ballistic Penrose process.

We present the basic assumptions. We consider the classical ballistic Penrose process, namely the decay of an in-going massive particle '0' in the ergosphere of a Kerr BH (usually with initial kinetic energy zero at infinite distance), into two particles '1' and '2' with masses

$$\mu_0,\ \ \mu_1,\ \ \mu_2 :\ \mu_0 > \mu_1 + \mu_2, \tag{3.1}$$

where μ_1 can be zero as described in the appendix B. After decay, the particle '1' counterrotates with the BH and is in a negative energy state as measured from an infinite distance. Meanwhile, particle '2' returns to infinity with mass energy of E_2, which is larger than that of the ingoing particle, E_0, potentially resulting in the extraction of rotational energy from the BH. Following the work of Ruffini and Wheeler [32], we assume that the test-particle approximation holds and decay happens at a turning point. Furthermore, the motion of test particles in the equatorial plane is considered, thus the motion is governed by an effective potential.

The effective potential is described in detail in the appendix A. For massive particles, for example, the effective potential is given by

$$\frac{V}{\mu} = \frac{2\hat{a}\hat{p}_\phi \pm \sqrt{\hat{r}\left[\hat{a}^2 + \hat{r}(\hat{r}-2)\right]\left(\hat{p}_\phi^2\hat{r} + \left[\hat{r}^3 + \hat{a}^2(2+\hat{r})\right]\right)}}{\hat{r}^3 + \hat{a}^2(\hat{r}+2)}, \tag{3.2}$$

that allows analyzing the physical trajectories on the equatorial plane of test particles with conserved energy E. The allowed regions for a particle of E are the regions with $V \leqslant E$, and the turning points occur where $V = E$ [33]. The above equation introduces dimensionless quantities for the BH, $\hat{a} = J/M^2$, and for a massive test particle, $\hat{E} = E/\mu$, $\hat{p}_\phi = p_\phi/(M\mu)$ and $\hat{r} = r/M$. Here, M and J are the BH mass and angular momentum, μ and p_ϕ are the test-particle rest mass and angular momentum, and r is the radial coordinate. In this study, only the positive sign solution in equation (3.2) is considered, deferring discussion of the negative sign solution for future analysis. For the positive sign solution and particle motion outside the event horizon ($\hat{r} > \hat{r}^+ = 1 + \sqrt{1-\hat{a}^2}$), an important property is revealed by the effective potential:

$$\hat{E} > \frac{\hat{a}\hat{p}_\phi}{2 + 2\sqrt{1-\hat{a}^2}}. \tag{3.3}$$

If precisely on the event horizon, the inequality above becomes equality, but this can never occur for the Penrose process because if a particle decays on the event horizon, no particle can escape. Therefore, only inequality will be utilized in the subsequent analysis.

There are some notes in the above assumptions. Since the minimum energy of a particle is achieved when $p_r = p_\theta = 0$ [33], we analyze the decay of a particle at the turning point. Moreover, the equations (see in the appendix B) are simplified when decay occurs at the turning

point; otherwise, the situation becomes more intricate due to the increase in free parameters. For the same reason, this process occurs on the equatorial plane, where the ergosphere reaches its maximum width, and where the effective potential for particle motion exists. Additionally, the sum of the two masses in equation (3.1), $\mu_1 + \mu_2$, cannot be equal to the initial particle mass μ_0 in this process. If the masses remain equal, the solution of trajectories of μ_1 and μ_2 always coincide, and they do not separate, meaning that these two particles never have a relative velocity. From a physical perspective, mass loss is necessary to generate kinetic energy in the center of the mass frame, allowing the two particles to have a relative velocity and separate.

Now, we utilize the equations to describe the scenario in which test particle '1' and particle '2' are created through the decay of particle '0' at a turning point in the ergosphere of a Kerr BH.

The equations controlling the decaying processes are described in detail in the appendix B. In generally, by setting values of $\hat{r}$, E_1 and $p_{\phi 1}$ that fulfill

$$\hat{r}: \ \hat{r}_+ < \hat{r} < 2 \tag{3.4a}$$

$$E_1 < 0, \ \ p_{\phi 1} < 0: \ E_1 > \frac{\hat{a}\frac{p_{\phi 1}}{M}}{2 + 2\sqrt{1-\hat{a}^2}}, \tag{3.4b}$$

and masses that satisfy equation (3.1), one can always find the corresponding positive values of geodesic conserved dimensionless quantities $\hat{E}_0$, $\hat{p}_{\phi 0}$, $\hat{E}_2$, and $\hat{p}_{\phi 2}$ from the set of equations:

$$\hat{p}_{r0} = 0, \tag{3.5a}$$

$$\mu_0 \hat{E}_0 = E_1 + \mu_2 \hat{E}_2, \tag{3.5b}$$

$$\mu_0 \hat{p}_{\phi 0} = p_{\phi 1} + \mu_2 \hat{p}_{\phi 2}, \tag{3.5c}$$

$$\mu_0 \hat{p}_{r0} = p_{r1} + \mu_2 \hat{p}_{r2}. \tag{3.5d}$$

Equation (3.5*a*) guarantees that the particle '0' decays at the turning point, equations (3.5*b*)–(3.5*d*) represents the conservation of energy, angular momentum, and radial momentum. For massive particle '1', E_1 and $p_{\phi 1}$ can expressed as dimensionless quantities $E_1 = \mu_1 \hat{E}_1$ and $p_{\phi 1} = \mu_1 \hat{p}_{\phi 1}$.

When particle '1' with negative energy and negative angular momentum falls into the BH, it reduces the mass and angular momentum of the BH according to

$$\Delta M = E_1 \tag{3.6}$$

and

$$\Delta J = p_{\phi 1}, \tag{3.7}$$

respectively. The energy extracted from the BH by particle '2' can be expressed as

$$E_{\text{extracted}} = \hat{E}_2 \mu_2 - \hat{E}_0 \mu_0. \tag{3.8}$$

According to the conservation of energy principle (i.e. equation (3.5*b*)), it can obtain

$$E_{\text{extracted}} = -E_1 = -\Delta M. \tag{3.9}$$

By solving equation (3.5) with a chosen set of parameters and utilizing the effective potential, examples of Penrose processes can be conveniently demonstrated. Usually, the parameters are chosen so that particle '0' drops from rest at infinity. But it should be noted that the specific energy of particle '0' ($\hat{E}_0$) can be equal to, larger than, or smaller than 1. Some specific examples can be found in section 5.

When the Penrose process occurs and the decay point coincides with the turning point on the equatorial plane, the decay position of the Penrose process can be constrained.

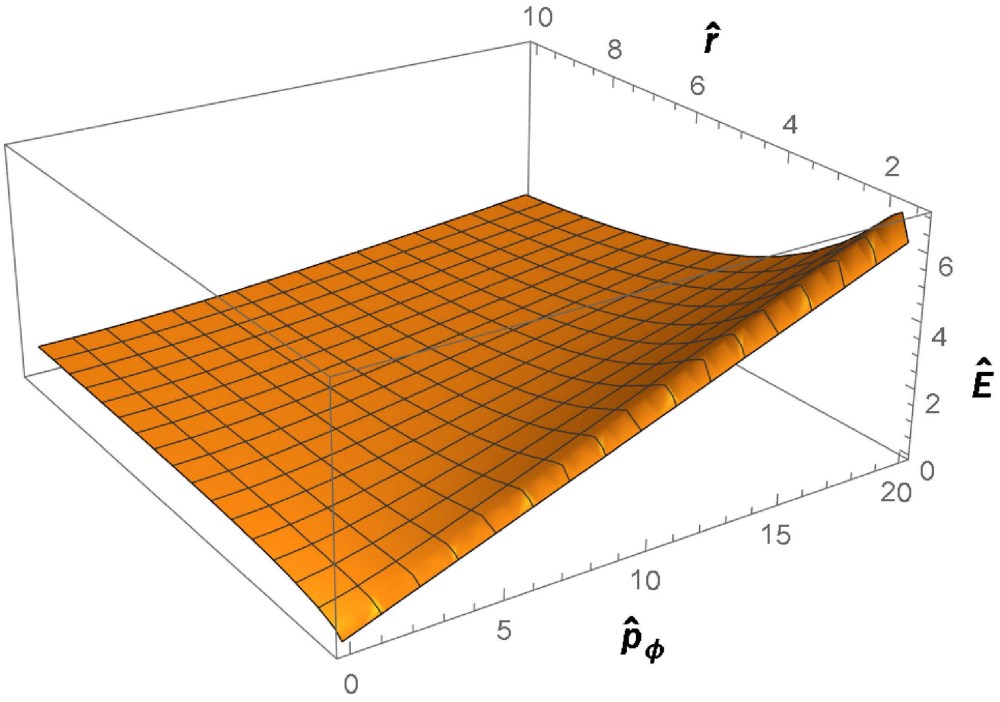

Figure 2. The effective potential of the massive test particle motion on the equatorial plane of Kerr space-time. A BH with spin $\hat{a} = 0.9$ is chosen. This figure shows the case of particles with positive angular momentum ($\hat{p}_\phi > 0$) outside the event horizon ($\hat{r} > \hat{r}_+$). The effective potential has a peak near the event horizon.

As depicted in the panels corresponding to particle '0' and particle '2' in figures 7 and 9, the presence of a turning point is evident when the effective potential exhibits a peak outside (or at) the event horizon. Otherwise, the effective potential monotonically decreases outside the horizon as $\hat{r}$ decreases. In this case, the particles at the turning point cannot escape outward. Additionally, for particle '2' to escape to infinity, the peak value of the effective potential should exceed 1. The position of this peak, denoted as $\hat{r}_{\rm peak}$, can be determined by

$$\frac{{\rm d}V}{{\rm d}\hat{r}}(\hat{r}_{\rm peak}) = 0. \tag{3.10}$$

Both particle '0' and particle '2' can only move at positions where $\hat{r} > \hat{r}_{\rm peak}$, indicating that the decay point occurs outside of $\hat{r}_{\rm peak}$. Any decay point inside of $\hat{r}_{\rm peak}$ is considered non-physical (refer to the example in the section 5). Figure 2 also illustrates the effective potential of the massive particle as a function of $\hat{r}$ and $\hat{p}_\phi$. Without loss of generality, $\hat{a} = 0.9$ is selected in figure 2 as an example. It is observed that $\hat{r}_{\rm peak}$ decreases monotonically with an increase in $\hat{p}_\phi$, and as $\hat{p}_\phi$ tends to infinity, $r_{\rm peak}$ approaches $\hat{r}_{\rm peak,\,min}$, i.e.

$$\hat{r}_{\rm peak,min} = \lim_{\hat{p}_\phi \to \infty} \hat{r}_{\rm peak}. \tag{3.11}$$

The value of $\hat{r}_{\rm peak,\,min}$ is solely dependent on the spin, as depicted in figure 3. It is evident that when $\hat{a} < \frac{1}{\sqrt{2}}$, $\hat{r}_{\rm peak,\,min} > 2$, which lies beyond the outer radius of the ergosphere of a Kerr BH. This implies that when $\hat{a} < \frac{1}{\sqrt{2}}$, the decay point cannot reside within the ergosphere, thus

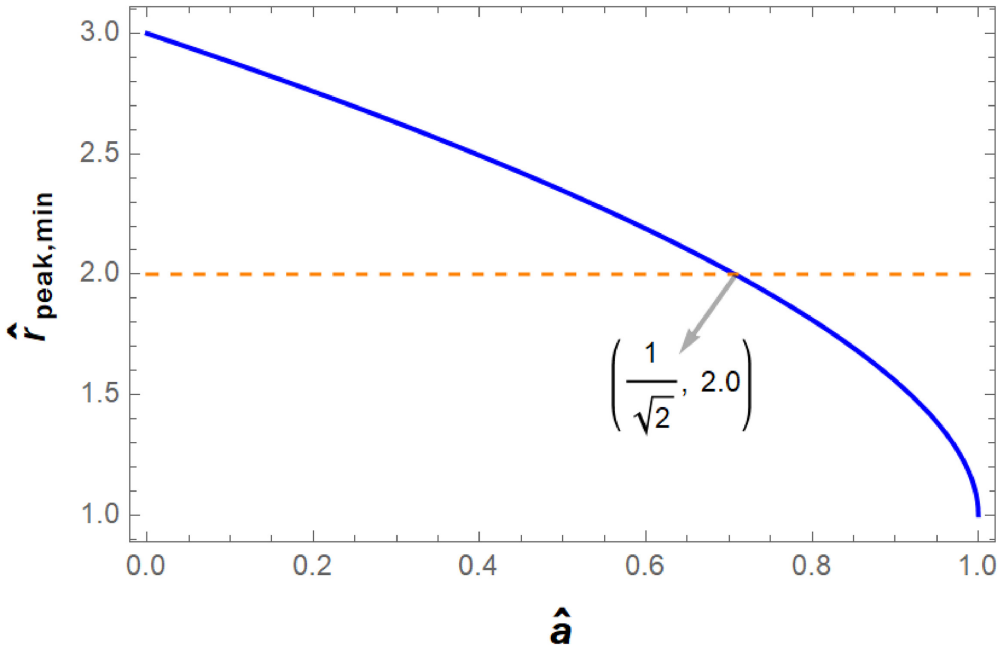

Figure 3. The value of $\hat{r}_{\text{peak,min}}$ is defined in equation (3.11) as a function of the dimensionless spin of the BH (blue curve). The orange dashed line indicates the outer radius of the ergosphere.

rendering the Penrose process impossible. Consequently, we will focus solely on the scenario where $\hat{a} > \frac{1}{\sqrt{2}}$ from now on.

4. Feedback on irreducible mass for extreme Kerr BH

Up until now, what has remained incomplete is the consideration of the feedback on the irreducible mass resulting from the capture of the counterrotating test particle by the BH horizon. In other words, it involves estimating the amount of rotational energy lost by the Kerr BH through the occurrence of this energy extraction process. We initiate the discussion by examining the case of an extreme Kerr BH in this section.

The general formula of change of irreducible mass after a Kerr BH absorbed a test particle is in appendix C. For the extreme Kerr BH ($\hat{a} = 1$), the change in irreducible mass after the absorption of test particle '1' with negative energy $E_1 = \hat{E}_1\mu_1$ and negative angular momentum $p_{\phi_1} = \hat{p}_{\phi 1}M\mu_1$ is given by:

$$\Delta M_{\text{irr}} = \sqrt{\left(M + \hat{E}_1\mu_1\right)^2 + \sqrt{\left(M + \hat{E}_1\mu_1\right)^4 - \left(M^2 + \hat{p}_{\phi 1}M\mu_1\right)^2}/\sqrt{2} - M/\sqrt{2}}. \tag{4.1}$$

The aim is to compare this quantity with the energy extracted from a BH. Thus, the following conditions can be checked:

$$\Delta M_{\text{irr}} > \mid \hat{E}_1 \mid \mu_1. \tag{4.2}$$

Table 1. The change of BH angular momentum, the change of BH mass, the change of irreducible mass, their ratio, and the change of transformable energy at different μ_1/M. We keep $\hat{r}=1.5$, $\hat{E}_1=-1.7935$, $\hat{p}_{\phi 1}=-10$, and the ratio is maintained as $\mu_0:\mu_1:\mu_2=2.4428:0.1:0.4$.

$\mu_1[M]$	$\Delta J=p_{\phi 1}[M^2]$	$\Delta M=E_1[M]$	$\Delta M_{\rm irr}[M]$	$\frac{\Delta M_{\rm irr}}{\lvert E_1\rvert}$	$\Delta E_{\rm trans}[M]$
10^{-2}	-0.1	-1.7935×10^{-2}	0.1026	5.7181	-0.1205
10^{-3}	-0.01	-1.7935×10^{-3}	0.0376	20.9904	-0.0394
10^{-6}	-10^{-5}	-1.7935×10^{-6}	1.2638×10^{-3}	704.6711	-1.2656×10^{-3}
10^{-57}	-10^{-56}	-1.7935×10^{-57}	4.0041×10^{-29}	2.2326×10^{28}	-4.0041×10^{-29}
0	0	0	0	∞	0

We introduce the quantity:

$$x_1=\mu_1/M, \tag{4.3}$$

and rewrite inequality (4.2) as:

$$\sqrt{\left(1+\hat{E}_1x_1\right)^2+\sqrt{\left(1+\hat{E}_1x_1\right)^4-(1+\hat{p}_{\phi_1}x_1)^2}}/\sqrt{2}-1/\sqrt{2}>|\hat{E}_1|x_1 \tag{4.4}$$

for $x_1\ll 1$ one can make power expansion in the left-hand side of (4.4) and get:

$$\frac{1}{2}\sqrt{x_1}\sqrt{2\hat{E}_1-\hat{p}_{\phi_1}}+\frac{1}{8}x_1\left(2\sqrt{2}\hat{E}_1+\sqrt{2}\hat{p}_{\phi_1}\right)>|\hat{E}_1|x_1, \tag{4.5}$$

or:

$$\frac{1}{2}\sqrt{2\hat{E}_1-\hat{p}_{\phi_1}}/\sqrt{x_1}+\frac{1}{8}\left(2\sqrt{2}\hat{E}_1+\sqrt{2}\hat{p}_{\phi_1}\right)>|\hat{E}_1|. \tag{4.6}$$

It is clear that for small x_1 this inequality tends to the inequality $\hat{E}_1>\hat{p}_{\phi_1}/2$. Thus, the following theorem is obtained:

$$\text{if } \mu_1\ll M \text{ then } \Delta M_{\rm irr}>|\hat{E}_1|\mu_1, \tag{4.7}$$

or: for any given $\hat{E}_1<0$ and $\hat{p}_{\phi_1}<0$, there exist $\mu_1<M$ such that $\Delta M_{\rm irr}>|\hat{E}_1|\mu_1$. Even more, for any given $\hat{E}_1<0$ and $\hat{p}_{\phi_1}<0$, there exist $\mu_1<M$ such that $\Delta M_{\rm irr}>h|\hat{E}_1|\mu_1$, where h is a any positive number.

When $\mu_1\to 0$, although the above proof represents the limit for massless particles, a more rigorous proof for massless particles is additionally adopted. The proof process for massless particles is similar to that of mass particles, but it should be noted that the energy and angular momentum of massless particles cannot use dimensionless quantities.

In table 1 we present some numerical examples corresponding to different μ_1/M ratios. Note that we regard μ_0,μ_1, and μ_2 as test particles. We adopt the test particle approximation for particles with mass satisfying $\mu/M<10^{-2}$. Therefore, as long as the ratio of μ_0,μ_1, and μ_2 are kept fixed, their dimensionless solutions from equations (3.5) are the same. From these examples, it follows that the absolute value of $\Delta E_{\rm trans}$ becomes smaller and smaller and

tends to 0 as μ_1/M decreases, $|\Delta E_{\rm trans}|/|E_1|$ becomes larger and larger and tends to infinity, standing equation (4.7). In the natural and reasonable range where $\mu_1/M \ll 1$, the conditions $\Delta M_{\rm irr}/|E_1| \gg 1$ and $|\Delta E_{\rm trans}| \gg |E_1|$ always hold. For the sake of rationality, in the subsequent analysis, we focus exclusively on the scenario where the mass of the test particle is significantly smaller than the mass of the BH, particularly in the case where $\mu_1/M \to 0$. For massless particles, the corresponding situation is considered where $|\frac{E_1}{M}| \to 0$ and $|\frac{p_{\phi 1}}{M^2}| \to 0$.

In short, for the Penrose process in an extreme Kerr BH, whether it involves a massive particle or a massless particle falling into the BH, the amount of extracted energy from a Kerr BH is much lower than the change in irreducible mass, resulting in high irreversibility and a significant shrinkage of transformable energy.

5. Feedback on irreducible mass for general Kerr BH

Even in discussions regarding general Kerr BHs, the condition of $\hat{a} > \frac{1}{\sqrt{2}}$ continues to be considered, as specified in the restrictions outlined in the last part of section 3.

As shown in appendix C, the change in the irreducible mass of a general Kerr BH after absorbing the test particle '1' is given by:

$$\Delta M_{\rm irr} = \sqrt{\left(M+\hat{E}_1\mu_1\right)^2 + \sqrt{\left(M+\hat{E}_1\mu_1\right)^4 - \left(\hat{a}M^2+\hat{p}_{\phi_1}M\mu_1\right)^2}}/\sqrt{2} - M\sqrt{1+\sqrt{1-\hat{a}^2}}/\sqrt{2}. \tag{5.1}$$

Similar to the example of an extreme BH, we aim to verify the following condition:

$$\Delta M_{\rm irr} > h|\hat{E}_1|\mu_1, \tag{5.2}$$

here, h is currently an arbitrary positive constant, but its corresponding relationship with $\hat{a}$ will be established in the subsequent analysis.

The quantity $x_1 = \mu_1/M$ can be introduced, and inequality (5.2) can be rewritten as:

$$\sqrt{\left(1+\hat{E}_1x_1\right)^2 + \sqrt{\left(1+\hat{E}_1x_1\right)^4 - \left(\hat{a}+\hat{p}_{\phi_1}x_1\right)^2}}/\sqrt{2} - \sqrt{1+\sqrt{1-\hat{a}^2}}/\sqrt{2} > h|\hat{E}_1|x_1 \tag{5.3}$$

for $x_1 \ll 1$ one can make power expansion in the left-hand side of equation (5.3) and get:

$$\frac{2\hat{E}_1 + \frac{2\hat{E}_1 - \hat{a}\hat{p}_{\phi_1}}{\sqrt{1-\hat{a}^2}}}{2\sqrt{2}\sqrt{1+\sqrt{1-\hat{a}^2}}}x_1 + O\left(x_1^2\right) > h|\hat{E}_1|x_1, \tag{5.4}$$

or

$$\frac{1+\frac{1}{\sqrt{1-\hat{a}^2}}}{\sqrt{2+2\sqrt{1-\hat{a}^2}}}\left(\hat{E}_1 - \frac{\hat{a}\hat{p}_\phi}{2+2\sqrt{1-\hat{a}^2}}\right)x_1 + O\left(x_1^2\right) > h|\hat{E}_1|x_1. \tag{5.5}$$

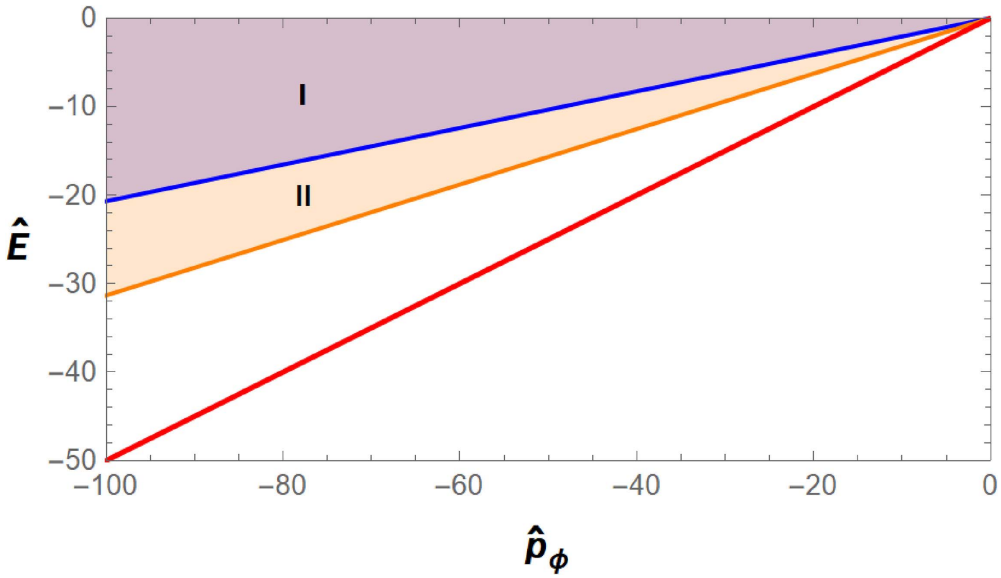

Figure 4. The region given by equations (5.5) and (5.6). The blue line gives the boundary of equation (5.5), and the orange line gives the boundary of equation (5.6). $\hat{a} = 0.9$ has been chosen here. When $\hat{a} = 1$, the regions given by equation (5.5) and equation (5.6) coincide, and the red solid line indicates their boundary.

While the inequality (3.3) is currently valid for any position outside the horizon, thus, we are able to demonstrate:

$$\frac{2\hat{E}_1 + \frac{2\hat{E}_1 - \hat{a}\hat{p}_{\phi_1}}{\sqrt{1-\hat{a}^2}}}{2\sqrt{2}\sqrt{1+\sqrt{1-\hat{a}^2}}} x_1 > 0. \tag{5.6}$$

However, we are unable to prove the equation (5.4) as we did in the last section.

Set $\hat{a} = 0.9$ and given $h = 1$, the regions given by inequalities (5.5) and (5.6) are shown in figure 4. The blue line represents the boundary of inequality (5.5), and the orange line represents the boundary of inequality (5.6), corresponding to the event horizon where the inequality (5.6) becomes equality. That is, region I satisfies $\Delta M_{\rm irr} > |E_1|$, while region II has $\Delta M_{\rm irr} < |E_1|$. Indeed, an extreme Kerr BH offers a fortunate case where the condition $\Delta M_{\rm irr} > |E_1|$ can be reduced to $\hat{E}_1 > \hat{p}_{\phi 1}/2$, resulting in the coincidence of the two boundary lines, as depicted in the red line. However, the same advantageous feature is not present for a non-extreme Kerr BH. The region where $\Delta M_{\rm irr} > |E_1|$ becomes significantly constrained. Nevertheless, further limitations on the irreducible mass feedback can be explored according to the location constraints of the Penrose process.

The main objective of the following analysis is to find the lower limit of irreducible mass feedback (as a function of BH spin) in the Penrose process.

We begin with the extension of figure 4, transforming it into a 3D depiction. First, we note that the effective potential given by equation (3.2) depends on the radius, whereas equation (5.5) does not contain radius. The boundary of equation (5.5) is

$$\frac{1+\frac{1}{\sqrt{1-\hat{a}^2}}}{\sqrt{2+2\sqrt{1-\hat{a}^2}}}\left(\hat{E}_1 - \frac{\hat{a}\hat{p}_{\phi}}{2+2\sqrt{1-\hat{a}^2}}\right) = h|\hat{E}_1|, \tag{5.7}$$

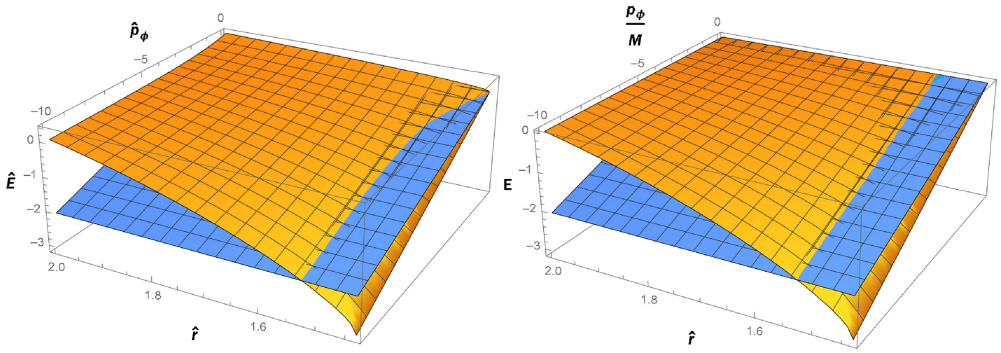

Figure 5. The effective potential surface (shown in orange), and the plane representing the increase in irreducible mass equal to the decrease in BH mass, i.e. equation (5.7) (shown in blue). The **left panel** illustrates the case of a massive particle, with the corresponding effective potential surface described by equation (3.2), while the **right panel** depicts the scenario of a massless particle, with the corresponding effective potential surface described by equation (A.9). The figure is drawn within the energy ergosphere ($\hat{r}^+ < \hat{r} < 2$), and for particles with negative angular momentum ($p_\phi < 0$), a BH spin of $\hat{a} = 0.9$ is selected.

from which one can express $\hat{E}_1$ as a function of $\hat{p}_\phi$. This function can be plotted as a plane. The intersection curve between this plane and the effective potential surface corresponds to the values of $\hat{r}$, denoted as $\hat{r}_{\rm crit}$. This 3D depiction and its intersection are shown in figure 5. For massive particles, $\hat{r}_{\rm crit}$ is a function of $\hat{p}_\phi$, while for massless particles, $\hat{r}_{\rm crit}$ is a constant related to $\hat{a}$. Selecting the radius $\hat{r}$ at the event horizon ($r = r_+$) on figure 5 will give the boundary lines on figure 4. The region where particles can move is situated above the effective potential surface (orange surface), coinciding with the orange surface when particles reach the turning point. The region above the blue plane signifies $\Delta M_{\rm irr} > |E_1|$, while the area below the blue plane indicates $\Delta M_{\rm irr} < |E_1|$.

The $\hat{r}_{\rm crit}(\hat{p}_\phi)$ corresponding to the intersection curve in figure 5 can be solved using the combined equations (3.2) and (5.7). For negative $\hat{p}_\phi$ values, $\hat{r}_{\rm crit}$ is a monotonically increasing function as $\hat{p}_\phi$ decreases. When $\hat{p}_\phi = 0$, $\hat{r}_{\rm crit} = r_+$, and when $\hat{p}_\phi$ approaches negative infinity, $\hat{r}_{\rm crit}$ approaches $\hat{r}_{\rm crit,max}$. In the case of massless particles, $\hat{r}_{\rm crit}$ remains a constant value independent of p_ϕ and precisely matches the $\hat{r}_{\rm crit,max}$ value of massive particles. $\hat{r}_{\rm crit,max}$ is solely dependent on the values of a and h. For a specific value such as $\hat{a} = 0.9$ and $h = 1$, the corresponding $\hat{r}_{\rm crit,max}$ is 1.53. In short, any position that violates $\Delta M_{\rm irr} < |E_1|$ cannot exceed $\hat{r}_{\rm crit,max}$, i.e. the condition $\Delta M_{\rm irr} < |E_1|$ can only occur within a limited region where $\hat{r}$ is smaller than $\hat{r}_{\rm crit,max}$, particularly in proximity to the horizon.

On the other hand, recalling the limit value $\hat{r}_{\rm peak,min}(\hat{a})$ that was determined in section 3, we equate these two limits, i.e.

$$\hat{r}_{\rm peak,min}\left(\hat{a}\right) = \hat{r}_{\rm crit,max}\left(\hat{a}, h\right). \tag{5.8}$$

By doing so, $h(\hat{a})$ can be solved as the lower limit of the increase in irreducible mass, providing the constraint on the irreducible mass feedback. This is because any physically valid solution for the decay point lies outside $\hat{r}_{\rm peak,min}$, equated to $\hat{r}_{\rm crit,max}$. Consequently, $\Delta M_{\rm irr} > h|E_1|$ holds for any physically valid solution (above the blue plane in the example of $h = 1$). The function of h with respect to $\hat{a}$ is numerically solved, as illustrated in figure 6. Therefore, the restriction on the growth of irreducible mass in the Penrose process is derived as $\Delta M_{\rm irr} > h|\Delta M|$.

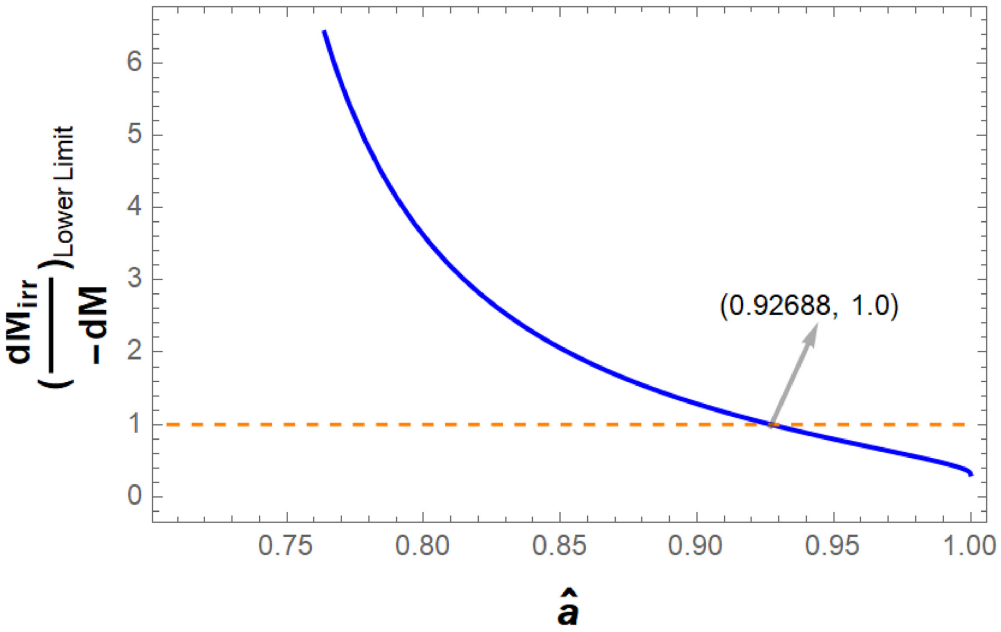

Figure 6. Restrictions on irreducible mass feedback for different spin of the BH, i.e the lower limit of increased irreducible mass as function of dimensionless spin from equation (5.8). The assumptions needed for this constraint are that these particles are test particles, and particle '0' decays at the turning point (while there is no need for particles '1' and '2' to be at the turning points).

As $\hat{a}$ approaches $\frac{1}{\sqrt{2}}$, h tends to infinity; however, in this case, the Penrose process can only occur at the outer boundary of the ergosphere. When $\hat{a}$ is less than 0.926 88, h is greater than 1, indicating that the Penrose process is highly irreversible for values of below 0.926 88. As $\hat{a}$ approaches 1, h approaches 0. However, it is important to note that when $\hat{a}$ equals 1, the restrictions obtained in this section are invalid, and the discussion in section 4 should be referred to.

In summary, for the Penrose process occurring in a general Kerr BH, when the decay point coincides with the turning point, we can not only constrain the decay position (as shown in figure 3), but also impose a restriction on the irreducible mass feedback, $\Delta M_{\rm irr} > h|\Delta M|$, where h is a function of $\hat{a}$ as depicted in the figure 6. Based on this differential relationship, it can be further calculated that a maximum of 11.6117% M of energy can be extracted, rather than 29.2893% M. It is noteworthy that the above proof remains applicable in the case where particle '1' is a massless particle, as $\hat{r}_{\rm crit,max}$ serves as the critical radius for massless particles.

We have already given the general restrictions on irreducible mass feedback of the Penrose process. Now, we present several illustrative examples to improve understanding of the Penrose process in general Kerr BH and its impact on the irreducible mass.

The first case is for $\hat{a} = 0.9$ and decay point of $\hat{r} = 1.75$. The schematic diagram and corresponding parameters are presented in figure 7, and the corresponding irreducible mass feedback is summarized in the first row of values in table 2. It is noteworthy that the effective potential peaks associated with particle '0' and particle '2' are both located to the left of the decay point, indicating the physical validity of this set of solutions. Furthermore, the increase in irreducible mass exceeds the decrease in the BH mass.

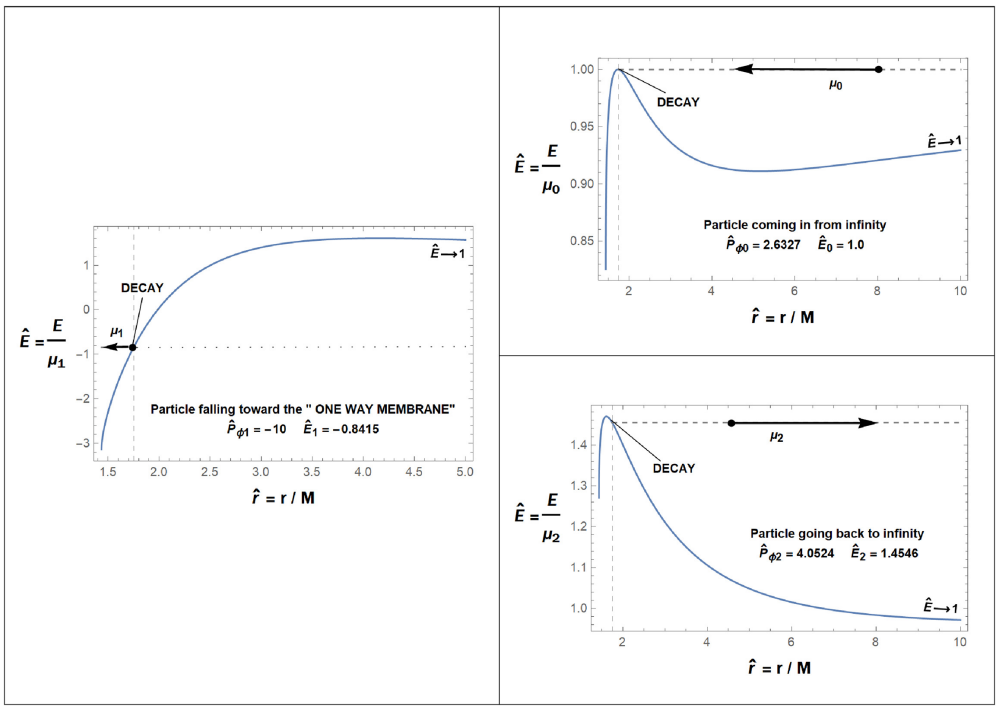

Figure 7. The physically feasible solution for particle '0' and particle '2' in region I of the left panel of figure 6. This process is highly irreversible ($\Delta M_{\rm irr} > \mid E_1 \mid$). In the example, $\hat{a}=0.9, \hat{r}=1.75$ is maintained, and the ratio is kept as $\mu_0:\mu_1:\mu_2=1:0.02:0.6990$.

Table 2. The summary of irreducible mass feedback when the mass of the test particle $\mu/M\to 0$. The columns, from left to right, represent the case number, the dimensionless spin of the BH, the location of the decay point, the ratio between the growth of irreducible mass and extracted energy in the limit of $\mu/M\to 0$, and a judgment of whether it is a physical solution. For the remaining parameters, please refer to the values in the corresponding case diagram.

Case	$\hat{a}$	$\hat{r}$	$\frac{\Delta M_{\rm irr}}{\mid E_1 \mid}$	physical solution?
1	0.9	1.75	$5.2955>1$	Yes
2	0.9	1.5	$0.7109<1$	No
3	0.98	1.27	$0.8962<1$	Yes

The second case is still for $\hat{a}=0.9$ but the decay point of $\hat{r}=1.5$. The schematic diagram and corresponding parameters are presented in figure 8, and the corresponding irreducible mass feedback is summarized in the second row of values in table 2. Although the expected increase in irreducible mass is smaller than the decrease in the BH mass, the effective potential peaks associated with particle '0' and particle '2' are both located to the right of the decay point, indicating that these particles would need to overcome the potential barrier to reach the decay point or escape to infinity. As a result, this set of solutions is considered non-physical in classical theory. However, it is possible that the solutions may become physically meaningful

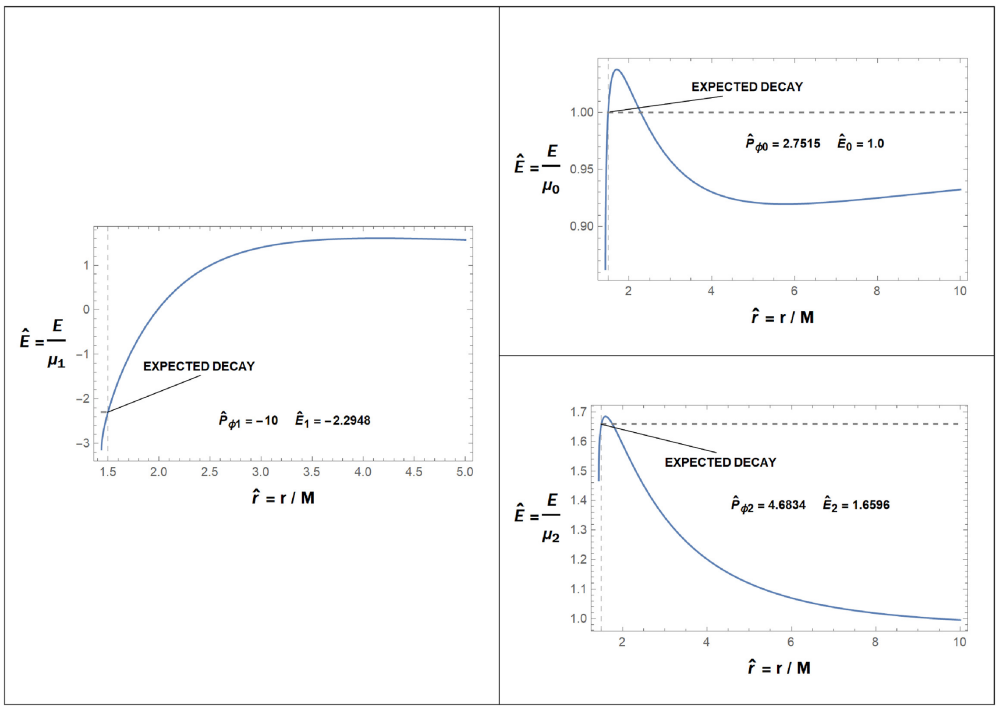

Figure 8. The nonphysical solution of particle '0' and particle '2' in region II of the left panel of figure 4. This process is not expected to be a highly irreversible process ($\Delta M_{\rm irr} <\mid E_1 \mid$). The vertical dashed line is the position where the particle '0' is expected to decay. In the example, $\hat{a} = 0.9, \hat{r} = 1.5, \hat{E}_1 = -2.2948, \hat{p}_{\phi 1} = -10$ is maintained, and the ratio kept as $\mu_0 : \mu_1 : \mu_2 = 1 : 0.02 : 0.6302$.

when accounting for the quantum effects of the particles. Nonetheless, discussing the quantum effects is beyond the scope of this paper.

The third one is for $\hat{a} = 0.98$ and the decay point of $\hat{r} = 1.27$. The schematic diagram and corresponding parameters are presented in figure 9, and the corresponding irreducible mass feedback is summarized in the third row of values in table 2. This case represents a physically valid solution, where the increase in irreducible mass is smaller than the decrease in the BH mass.

In the above examples, the first one represents a physical solution, while the second one corresponds to a non-physical solution. This distinction arises because the decay point in the first example is outside the $\hat{r}_{\rm peak,min}(\hat{a} = 0.9)$, while the decay point in the second example falls within the $\hat{r}_{\rm peak,min}(\hat{a} = 0.9)$. Both examples maintain $\hat{p}_\phi = -10$, resulting in relatively larger feedback on the irreducible mass in the first example due to the larger decay radius. Bringing the decay point closer to the event horizon reduces the feedback on the irreducible mass, but it may also lead to a non-physical solution, as observed in example 2. Moreover, particular attention should be given to example 3, which presents a physical solution where the increase in irreducible mass is smaller than the decrease in the BH mass. This suggests that the Penrose process is not consistently highly irreversible.

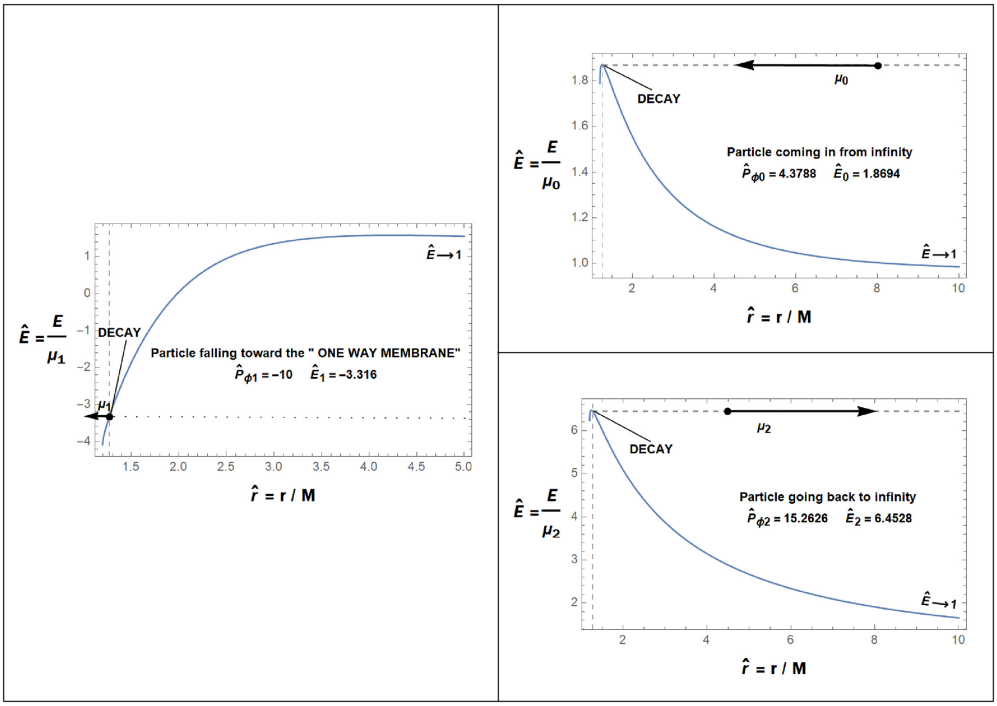

Figure 9. The physically feasible solution where the increase in irreducible mass is smaller than the decrease in the BH mass ($\Delta M_{\rm irr} < \mid E_1 \mid$), i.e. this process is not a highly irreversible process. In the example, $\hat{a} = 0.98$, $\hat{r} = 1.27$ is maintained, and the ratio kept as $\mu_0 : \mu_1 : \mu_2 = 1 : 0.02 : 0.3$.

6. Discussion and conclusions

Determining the increase in the irreducible mass of a BH is crucial, as it not only reflects the irreversibility of the corresponding process but also renders the calculation of changes in the surface area and BH entropy effortless. Moreover, the energy extraction process in a BH reduces the BH mass while increasing the irreducible mass, both of which lead to a contraction of the transformable energy. As a result, the total energy that can actually be extracted from a BH is less than what would have been possible if no feedback had been considered. For instance, Tursunov and Dadhich [31] indicate that all the initial transformable energy is available for extraction. However, our results show that the energy extraction process may be highly irreversible and result in significantly less energy being extractable from a BH compared to the initial transformable energy.

To illustrate the relationship between the released energy of a BH and the increase in its irreducible mass, the Penrose process is examined as an example. We have re-derived the fundamental equations describing test particle motion and decay on the equatorial plane of a Kerr BH, considering both massive and massless particles. These equations allow us to quantitatively demonstrate the feedback of irreducible mass.

In the case of an extreme Kerr BH, as the limit $\mu_1/M \to 0$ is approached, the ratio $\Delta M_{\rm irr}/|E_1|$ tends to infinity, indicating that all the reduced transformable energy contributes

to the increase in irreducible mass. This high irreversibility is demonstrated in table 1. The amount of energy extracted from a Kerr BH using massive particles is significantly lower than the change in transformable energy.

For non-extreme Kerr BHs, the effective potential of particle motion on the equatorial plane in Kerr spacetime is analyzed. It is demonstrated that only BHs with a dimensionless spin $\hat{a}$ greater than $1/\sqrt{2}$ can undergo the Penrose process if the decay point coincides with the turning point. Based on this analysis, the lower limit for the change in irreducible mass as a function of the BH's dimensionless spin is provided (figure 6).

There are numerous equally important processes for the case where the decay point does not coincide with the turning point, as well as for the analysis of the negative root solution in equation (3.2). The negative root solution may not be intuitively obvious from a physical standpoint. However, since it is also a solution of the Einstein field equations, it warrants further consideration. This may be related to the motion of antimatter in the reverse direction of time. Additionally, various energy extraction processes, such as the confined Penrose process [22], collisional Penrose processes [19], and the Blandford–Znajek(BZ) process [20], are worth studying in terms of their feedback to BHs. Furthermore, the Pollock process [29, 30] and accretion processes are also relevant for understanding the irreducible mass and irreversibility of BHs. These physical processes either involve consideration of BH magnetic fields (such as the BZ mechanism and Pollock process) or complex systems with many particles (such as collisional Penrose processes). When considering magnetic fields, not only may the magnetic field itself interact with the BH, altering its mass and irreducible mass, but it may also extend the ergosphere of the BH, leading to the appearance of a wider range of negative-energy orbits, thereby resulting in different energy extraction and feedback from the BH compared to the Penrose processes considered in the current manuscript. When considering complex multi-particle systems, we intend to statistically account for the energy extracted from the BH and the feedback on the BH, rather than considering the trajectory of each individual particle and its impact on the BH. These supplementary findings will be discussed in future research.

Data availability statement

All data that support the findings of this study are included within the article (and any supplementary files).

Acknowledgments

We thank Prof. R Ruffini, Prof. J A Rueda, and Prof. Yu Wang for the discussions on the topic of this work. S R Z acknowledges support from China Scholarship Council (CSC No. 202206340085).

Conflict of interest

The authors declare no relevant competing interests pertaining to the content of this article. Data sharing is not applicable to this article, as no datasets were generated or analyzed during the current study.

Appendix A. Effective potential

In this appendix, explicit formulas for quantities relevant to describing the Penrose process in Kerr spacetime are provided. In Boyer–Lindquist coordinates [34] and units where G = c = 1, the Kerr metric takes the form

$$\begin{aligned} \mathrm{d}s^2 &= g_{\alpha\beta}\mathrm{d}x^\alpha \mathrm{d}x^\beta \\ &= -\left(1 = \frac{2Mr}{\Sigma}\right)\mathrm{d}t^2 - \frac{4Mar\sin^2\theta}{\Sigma}\mathrm{d}t\mathrm{d}\phi + \frac{\Sigma}{\Delta}\mathrm{d}r^2 + \Sigma\mathrm{d}\theta^2 + \frac{A}{\Sigma}\sin^2\theta\mathrm{d}\phi^2 \end{aligned} \tag{A.1}$$

where M is the mass of the BH, $\hat{a} \equiv a/M = J/M^2$ is its dimensionless spin, and

$$\begin{aligned} &\Sigma \equiv r^2 + a^2\cos^2\theta, \\ &\Delta \equiv a^2 + r^2 - 2Mr, \\ &A = \left(r^2 + a^2\right)^2 - \Delta a^2\sin^2\theta. \end{aligned} \tag{A.2}$$

For a test particle, the four-momentum is

$$p^\alpha \equiv \mathrm{d}x^\alpha/\mathrm{d}\lambda = \left(\frac{\mathrm{d}t}{\mathrm{d}\lambda}, \frac{\mathrm{d}r}{\mathrm{d}\lambda}, \frac{\mathrm{d}\theta}{\mathrm{d}\lambda}, \frac{\mathrm{d}\phi}{\mathrm{d}\lambda}\right) \tag{A.3}$$

where λ is an affine parameter. The existence of a conserved energy, a conserved angular momentum, and a conserved rest mass of the particle

$$\begin{aligned} &E = -p_t, \\ &L_z = p_\phi, \\ &\mu = \left(-p^\alpha p_\alpha\right)^{\frac{1}{2}}. \end{aligned} \tag{A.4}$$

Dimensionless quantities can be introduced for convenience: $\hat{r} = r/M$, $\hat{a} = a/M$ and for massive particles additionally have the constants of motion: $\hat{E} = E/\mu$, $\hat{p}_\phi = p_\phi/M/\mu$. The ergosphere is maximal in the equatorial plane; therefore, the decay of a particle falling onto the BH in the equatorial plane is considered.

The motion of a particle (both mass particle and massless particle) in the equatorial plane of Kerr BH is governed by effective potential, which is given by

$$V(r) = \frac{\beta \pm \sqrt{\beta^2 - \alpha\gamma_0}}{\alpha}, \tag{A.5}$$

where α, β and γ_0 given by

$$\begin{aligned} &\alpha = \left(r^2 + a^2\right)^2 - \Delta a > 0 \\ &\beta = 2Mrap_\phi \\ &\gamma_0 = \left(r^2 - 2Mr\right)p_\phi^2 - \mu^2 r^2\Delta. \end{aligned} \tag{A.6}$$

Only the positive sign solution is considered in this paper. The allowed regions for a particle of E are the regions with $V \leqslant E$, and the turning points occur where $V = E$ [33].

For massive particle,

$$\frac{V}{\mu}=\frac{2\hat{a}\hat{p}_{\phi}+\sqrt{\hat{r}\left[\hat{a}^2+\hat{r}\left(\hat{r}-2\right)\right]\left(\hat{p}_{\phi}^2\hat{r}+\left[\hat{r}^3+\hat{a}^2\left(2+\hat{r}\right)\right]\right)}}{\hat{r}^3+\hat{a}^2\left(\hat{r}+2\right)}, \tag{A.7}$$

when $r\to r_+$, $\frac{V}{\mu}\to\frac{\hat{a}\hat{p}_{\phi}}{2+2\sqrt{1-\hat{a}^2}}$ where $r_+=M+\sqrt{M^2-a^2}$ is the radius of the outer horizon. Thus, we have that $\hat{E}>\frac{\hat{a}\hat{p}_{\phi}}{2+2\sqrt{1-\hat{a}^2}}$ for $\hat{r}>\hat{r}^+$. For the extreme Kerr BH ($a=M$),

$$\frac{V}{\mu}=\frac{2\hat{p}_{\phi}+\left(\hat{r}-1\right)\sqrt{\hat{r}\left(\hat{r}^3+\hat{r}+2\right)+\hat{p}_{\phi}^2\hat{r}^2}}{\hat{r}^3+\hat{r}+2}, \tag{A.8}$$

when $\frac{r}{M}\to 1$, $\frac{V}{\mu}\to\frac{\hat{p}_{\phi}}{2}$. Thus, we have that $\hat{E}>\frac{\hat{p}_{\phi}}{2}$ for $\hat{r}>\hat{r}^+=1$.

For massless particle,

$$V=\frac{2\hat{a}\frac{p_{\phi}}{M}+\hat{r}\sqrt{\left[\hat{a}^2+\hat{r}\left(\hat{r}-2\right)\right]\frac{p_{\phi}^2}{M^2}}}{\hat{r}^3+\hat{a}^2\left(\hat{r}+2\right)}, \tag{A.9}$$

when $r\to r_+$, $V\to\frac{\hat{a}\frac{p_{\phi}}{M}}{2+2\sqrt{1-\hat{a}^2}}$. Thus, we have that $E>\frac{\hat{a}\frac{p_{\phi}}{M}}{2+2\sqrt{1-\hat{a}^2}}$ for $\hat{r}>\hat{r}^+$. For the extreme Kerr BH,

$$V=\frac{\frac{2p_{\phi}}{M}+\hat{r}\left(\hat{r}-1\right)\sqrt{\frac{p_{\phi}^2}{M^2}}}{\hat{r}^3+\hat{r}+2}, \tag{A.10}$$

when $\frac{r}{M}\to 1$, $V\to\frac{p_{\phi}}{2M}$. Thus, have that $E>\frac{p_{\phi}}{2M}$ for $\hat{r}>\hat{r}^+=1$.

Appendix B. Particle decaying processes

We can imagine that test particle '1' was created by the decay of particle '0' at some turning point in the ergosphere of Kerr BH when particle '1' goes into the horizont and particle '2' goes out to infinity (Penrose process). Since the minimum energy of a particle is achieved when $p_r=p_{\theta}=0$ [33], we only analyze the decay of a particle at the turning point.

For any given

$$\hat{r}:\ \hat{r}_+<\hat{r}<2 \tag{B.1a}$$

$$E_1<0,\ \ p_{\phi 1}<0:\ E_1>\frac{\hat{a}\frac{p_{\phi 1}}{M}}{2+2\sqrt{1-\hat{a}^2}}. \tag{B.1b}$$

$$\mu_0,\ \ \mu_1,\ \ \mu_2:\ \mu_0>\mu_1+\mu_2, \tag{B.1c}$$

one can always find the corresponding positive values

$$\hat{E}_0,\ \ \hat{p}_{\phi 0},\ \ \hat{E}_2,\ \ \hat{p}_{\phi 2} \tag{B.2}$$

from the following set of equations:

$$\hat{p}_{r0}=0, \tag{B.3a}$$

$$\mu_0\hat{E}_0=E_1+\mu_2\hat{E}_2, \tag{B.3b}$$

$$\mu_0\hat{p}_{\phi 0}=p_{\phi 1}+\mu_2\hat{p}_{\phi 2}, \tag{B.3c}$$

$$\mu_0\hat{p}_{r0}=p_{r1}+\mu_2\hat{p}_{r2}, \tag{B.3d}$$

where

$$\hat{p}_{r0}=\left\{\left(\hat{E}_0^2-1\right)\hat{r}^3+2\hat{r}^2+\left[\hat{a}^2\left(\hat{E}_0^2-1\right)-\hat{p}_{\phi 0}^2\right]\hat{r}+2\left(\hat{a}\hat{E}_0-\hat{p}_{\phi 0}\right)^2\right\}^{1/2}, \tag{B.4}$$

$$\hat{p}_{r2}=\left\{\left(\hat{E}_2^2-1\right)\hat{r}^3+2\hat{r}^2+\left[\hat{a}\left(\hat{E}_2^2-1\right)-\hat{p}_{\phi 2}^2\right]\hat{r}+2\left(\hat{a}\hat{E}_2-\hat{p}_{\phi 2}\right)^2\right\}^{1/2}. \tag{B.5}$$

And the explicit expression of p_{r1} depends on whether particle '1' has mass or not. For massive particle '1', conserved quantities can be expressed in a dimensionless form and

$$\hat{p}_{r1}=-\left\{\left(\hat{E}_1^2-1\right)\hat{r}^3+2\hat{r}^2+\left[\hat{a}\left(\hat{E}_1^2-1\right)-\hat{p}_{\phi 1}^2\right]\hat{r}+2\left(\hat{a}\hat{E}_1-\hat{p}_{\phi 1}\right)^2\right\}^{1/2}. \tag{B.6}$$

For massless particle '1', conserved quantities cannot be expressed in a dimensionless form and

$$p_{r1}=-\left[E_1^2\hat{r}^3+\left(\hat{a}^2E_1^2-\frac{p_{\phi_1}^2}{M^2}\right)\hat{r}+2\left(\hat{a}E_1-\frac{p_{\phi_1}}{M}\right)^2\right]^{1/2}. \tag{B.7}$$

Equation (B.3*a*) guarantees that the particle '0' decays at the turning point (see example figure 7), equations (B.3*b*)–(B.3*d*) represents the conservation of energy, angular momentum, and radial momentum.

Furthermore, it is essential to note the following: 1) if we assume that the particle '1' is also generated at the turning point, we have $p_{r1}=0$, and as a consequence, $\hat{p}_{r2}=0$; 2) if particle '2' is massless, the physical quantity related to particle '2' should not be expressed as a dimensionless quantity, similar to the physical quantity associated with particle '1'.

Appendix C. Change of irreducible mass

Particular attention is given to the role of the irreducible mass. Inverting equation (1.1), the irreducible mass can be expressed as a function of the BH mass and angular momentum. There are two negative and two positive roots. For obvious reasons, the two negative roots are discarded, and the two positive roots are

$$M_{\rm irr}^{(\pm)}=\sqrt{\frac{M^2\pm\sqrt{M^4-J^2}}{2}}, \tag{C.1}$$

which for the extreme Kerr BH coincide, i.e.

$$M_{\rm irr}=M_{\rm irr}^{(+)}=M_{\rm irr}^{(-)}=\frac{M}{\sqrt{2}}. \tag{C.2}$$

Generally, only the plus sign root in equation (C.1) is physical, while the negative sign root is unphysical. For instance, the latter leads to $M_{\rm irr}^{(-)}(J=0)=0$, instead of the correct result, $M_{\rm irr}^{(+)}(J=0)=M$.

Now, we consider the change of irreducible mass of a Kerr BH after absorbing the particle '1' with energy E_1 and angler momentum $p_{\phi 1}$ from the equatorial plane:

$$\Delta M_{\rm irr}=\sqrt{\left(M+E_1\right)^2+\sqrt{\left(M+E_1\right)^4-\left(\hat{a}M^2+p_{\phi_1}\right)^2}}/\sqrt{2}-M\sqrt{1+\sqrt{1-\hat{a}^2}}/\sqrt{2}. \tag{C.3}$$

It is worth noting that the change in irreducible mass exhibits nonlinear behavior with respect to μ_1 in general. Moreover, in the case of a massive particle, the quantities E_1 and $p_{\phi 1}$ can be expressed as dimensionless values.

ORCID iD

Shu-Rui Zhang https://orcid.org/0000-0003-0368-384X

References

[1] Blandford R and Globus N 2022 Ergomagnetosphere, ejection disc, magnetopause in M87 - I. Global flow of mass, angular momentum, energy and current *Mon. Not. R. Astron. Soc.* **514** 5141
[2] Zaslavskii O B 2023 General properties of the Penrose process with neutral particles in the equatorial plane (arXiv:2307.06469)
[3] Kerr R P 1963 Gravitational field of a spinning mass as an example of algebraically special metrics *Phys. Rev. Lett.* **11** 237
[4] Carter B 1968 Global structure of the kerr family of gravitational fields *Phys. Rev.* **174** 1559
[5] Rees M, Ruffini R and Wheeler J A 1974 Black holes, gravitational waves and cosmology: an introduction to current research *Top. Astrophys. Space Phys.* **10** 64–65
[6] Landau L D 2013 *The Classical Theory of Fields* vol 2 (Elsevier)
[7] Ruffini R and Wheeler J A 1971 Introducing the black hole *Phys. Today* **24** 30
[8] Christodoulou D 1970 Reversible and irreversible transformations in black-hole physics *Phys. Rev. Lett.* **25** 1596–7
[9] Christodoulou D and Ruffini R 1971 Reversible transformations of a charged black hole *Phys. Rev.* D **4** 3552
[10] Hawking S W 1971 Gravitational radiation from colliding black holes *Phys. Rev. Lett.* **26** 1344–6
[11] Bekenstein J D 1973 Black holes and entropy *Phys. Rev.* D **7** 2333
[12] Ruffini R *et al* 2019 On the GeV emission of the type I BdHN GRB 130427A *Astrophys. J.* **886** 82
[13] Rueda J A and Ruffini R 2020 The blackholic quantum *Eur. Phys. J.* C **80** 300
[14] Moradi R, Rueda J A, Ruffini R and Wang Y 2021 The newborn black hole in GRB 191014C proves that it is alive *Astron. Astrophs.* **649** A75
[15] Rueda J A, Ruffini R and Kerr R P 2022 Gravitomagnetic interaction of a kerr black hole with a magnetic field as the source of the jetted GeV radiation of gamma-ray bursts *Astrophys. J.* **929** 56
[16] Bekenstein J D 1973 Extraction of energy and charge from a black hole *Phys. Rev.* D **7** 949
[17] Teukolsky S A and Press W H 1974 Perturbations of a rotating black hole. III. Interaction of the hole with gravitational and electromagnetic radiation *Astrophys. J.* **193** 443
[18] Ruffini R and Wilson J R 1975 Relativistic magnetohydrodynamical effects of plasma accreting into a black hole *Phys. Rev.* D **12** 2959
[19] Piran T, Shaham J and Katz J 1975 High efficiency of the penrose mechanism for particle collisions *Astrophys. J. Lett.* **196** L107
[20] Blandford R D and Znajek R L 1977 Electromagnetic extraction of energy from Kerr black holes *Mon. Not. R. Astron. Soc.* **179** 433
[21] Bekenstein J D and Schiffer M 1998 The many faces of superradiance *Phys. Rev.* D **58** 064014
[22] Zaslavskii O B 2022 Confined Penrose process and black-hole bomb *Phys. Rev.* D **106** 024037
[23] Rueda J and Ruffini R 2023 Extracting the energy and angular momentum of a kerr black hole (arXiv:2303.07760)
[24] Penrose R and Floyd R M 1971 Extraction of rotational energy from a black hole *Nat. Phys. Sci.* **229** 177
[25] Wald R M 1974 Energy limits on the penrose process *Astrophys. J.* **191** 231
[26] Chandrasekhar S 1998 *The Mathematical Theory of Black Holes* vol 69 (Oxford University Press)
[27] Camenzind M 2007 *Compact Objects in Astrophysics* (Springer)
[28] Zhang S-R 2023 The transformation of the rotational energy of an accreting kerr black hole *Astron. Rep.* **67** S97
[29] Pollock M 1976 The interaction between a weak magnetic field and a slowly rotating black hole *Proc. R. Soc.* A **350** 239

[30] King A R and Lasota J P 1977 Magnetic alignment of rotating black holes and accretion discs *Astron. Astrophs.* **58** 175
[31] Tursunov A and Dadhich N 2019 Fifty years of energy extraction from rotating black hole: revisiting magnetic penrose process *Universe* **5** 125
[32] Ruffini R and Wheeler J A 1971 Relativistic cosmology and space platforms *ESRO* **52** 45
[33] Misner C W, Thorne K S and Wheeler J A 1973 *Gravitation* (W. H. Freeman)
[34] Boyer R H and Lindquist R W 1967 Maximal analytic extension of the kerr metric *J. Math. Phys.* **8** 265